

- MULDER, F. & HUISZON, C. (1977). *Mol. Phys.* **34**, 1215–1235.
- MULLIKEN, R. S. (1955). *J. Chem. Phys.* **23**, 1833–1840.
- NEUMANN, D. B., BASCH, H., KORNEGAY, R. L., SNYDER, L. C., MOSKOWITZ, J. W., HORNBACH, J. & LIEBMANN, S. P. (1974). *Quantum Chemistry Program Exchange*, **10**, 199. Department of Chemistry, Indiana Univ., Bloomington, IN 47405, USA.
- POLITZER, P. & HARRIS, R. R. (1970). *J. Am. Chem. Soc.* **92**, 6451–6454.
- POPLE, J. A. (1980). Private communication.
- SCROCCO, E. & TOMASI, J. (1978). *Adv. Quantum Chem.* **11**, 115–193.
- SHOOLERY, J. N. & SHARBAUGH, A. H. (1951). *Phys. Rev.* **82**, 95.
- SMIT, P. H., DERISSEN, J. L. & VAN DUINEVELDT, F. B. (1977). *J. Chem. Phys.* **67**, 274–282.
- SMIT, P. H., DERISSEN, J. L. & VAN DUINEVELDT, F. B. (1979). *Mol. Phys.* **37**, 521–539.
- SNYDER, L. C. & BASCH, H. (1972). *Molecular Wavefunctions and Properties*. New York: Wiley.
- STARR, T. L. (1976). PhD Dissertation, Univ. of Louisville.
- STEINER, E. (1976). *The Determination and Interpretation of Molecular Wave Functions*. Cambridge Univ. Press.
- SUTOR, J. (1963). *J. Chem. Soc.* pp. 1105–1110.
- TROTTER, J. (1960). *Acta Cryst.* **13**, 86–95.
- WEISS, R. (1963). *Phys. Rev.* **131**, 659–665.
- WILLIAMS, D. E. (1971). *Acta Cryst.* **A27**, 452–455.
- WILLIAMS, D. E. (1979). *Quantum Chemistry Program Exchange*, **11**, 373. Department of Chemistry, Indiana Univ., Bloomington, IN 47405, USA.
- WILLIAMS, D. E. (1981). *Chem. Phys.* In the press.
- WILLIAMS, D. E. & STARR, T. L. (1977). *Comput. Chem.* **1**, 173–177.

Acta Cryst. (1981). **A37**, 301–308

The Superstructure of the Intermediate Pyrrhotite. II. One-Dimensional Out-of-Step Vector of Fe Vacancies in the Incommensurate Structure with Compositional Range from Fe_9S_{10} to $\text{Fe}_{11}\text{S}_{12}$

BY KICHIRO KOTO

Institute of Scientific and Industrial Research, Osaka University, Suita, Osaka, 565 Japan

AND MASAO KITAMURA*

Faculty of Science, Tohoku University, Aobayama, Sendai, 980 Japan

(Received 16 June 1980; accepted 1 November 1980)

Abstract

Satellite reflections appear parallel to c^* : only even and odd orders around main reflections with h and k both even and both odd, respectively, which are explained by assuming that two kinds of out-of-step vectors, such as $(\mathbf{a} + \mathbf{b})/4$ and $(\mathbf{a} - \mathbf{b})/4$, occur alternately at intervals of $c/4$ along the orthorhombic c axis. The main origin of the superstructure is the ordering of the Fe vacancies, the distribution of which in four different Fe rows parallel to the c axis is studied in terms of Fourier expansion.

Introduction

The intermediate pyrrhotite with the compositional range from Fe_9S_{10} (5C type) to $\text{Fe}_{11}\text{S}_{12}$ (6C type) has a superstructure of the NiAs type with various incommensurate c periods from 5 to 6 times as long as a sub-period (Morimoto, Gyobu, Tsukuma & Koto, 1975). Their lattices are orthorhombic C -centered with $\mathbf{a} = 2\mathbf{A}_1$, $\mathbf{b} = 2\mathbf{A}_1 + 4\mathbf{A}_2$ and $\mathbf{c} = N\mathbf{C}$ where \mathbf{A}_1 , \mathbf{A}_2 and \mathbf{C} represent the hexagonal subcell vectors of the NiAs type and N is generally incommensurate ($5 \leq N \leq 6$). $|\mathbf{A}_1|$ and $|\mathbf{A}_2| \sim 3.5$, and $|\mathbf{C}| \sim 5.7$ Å.

The 5C and 6C types are respectively commensurate with just 5 and 6 times the length of a sub-period. These are the limiting cases of the incommensurate types. In part I (Koto, Morimoto & Gyobu, 1975), the structure of the 6C type has been studied. The main origin of the superstructure is the ordering of Fe vacancies as in the 4C type, Fe_7S_8 (Bertaut, 1953). The structure of the 6C type is statistical and a filled layer of Fe atoms alternates with two consecutive partially defective layers along the c axis. The distribution of the Fe vacancies in the two structures of the 4C and 6C types is explained by a one-dimensional out-of-step vector at intervals of $c/4$ along the c axis, as shown in Fig. 1 (Koto, Morimoto &

The 5C and 6C types are respectively commensurate with just 5 and 6 times the length of a sub-period. These are the limiting cases of the incommensurate types. In part I (Koto, Morimoto & Gyobu, 1975), the structure of the 6C type has been studied. The main origin of the superstructure is the ordering of Fe vacancies as in the 4C type, Fe_7S_8 (Bertaut, 1953). The structure of the 6C type is statistical and a filled layer of Fe atoms alternates with two consecutive partially defective layers along the c axis. The distribution of the Fe vacancies in the two structures of the 4C and 6C types is explained by a one-dimensional out-of-step vector at intervals of $c/4$ along the c axis, as shown in Fig. 1 (Koto, Morimoto &

* Present address: Faculty of Science, Kyoto University, Sakyo-ku, Kyoto, 606 Japan.

Gyobu, 1975). Incommensurate superstructures of the intermediate pyrrhotite can be also explained in essentially the same way (Koto, Morimoto & Kitamura, 1975).

The fractional nature of the period was firstly confirmed theoretically by using the antiphase function or the step function (Fujiwara, 1957). Kakinoki & Minagawa (1972) refined Fujiwara's model and made some important remarks on the application of the step function, and Minagawa (1972) proposed an alternative model for the structure with an incommensurate value for the half period, \bar{M} .

In the present paper the diffraction aspect of the commensurate and incommensurate superstructures of the intermediate pyrrhotite is studied by using the step function, and relationships between the coefficients of the Fourier series which represents the distribution of Fe vacancy in the superstructure are obtained.

Diffraction aspect

One-dimensional out-of-step vector

Laue symmetry is mmm in the intensity distribution of the intermediate pyrrhotite. Satellite reflections appear parallel to c^* and are only even and only odd orders around main reflections with h and k both even and both odd, respectively, as shown schematically in Fig. 2. The fundamental structure of pyrrhotite is of the NiAs type and Fe atoms form a primitive lattice (Fig. 3). Because no vacancy is observed with S atoms, we

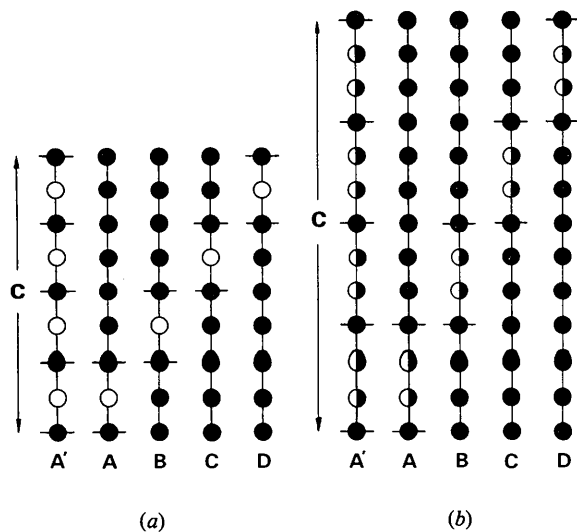


Fig. 1. Distribution of Fe vacancies in four different rows (A , B , C and D) for (a) the 4C-type Fe_7S_8 and (b) the 6C-type $\text{Fe}_{11}\text{S}_{12}$. The A prime row represents a hypothetical Fe row at A before the out-of-step vector occurs. This is the same as Fig. 5 of Koto, Morimoto & Gyobu (1975).

may, at first, take into account only the vacancies of Fe atoms in determining the origin of the satellite reflections. Fe atoms are at $(0,0,0)$ and $(0,0,\frac{1}{2})$ of the hexagonal lattice with A_1 , A_2 and C (Fig. 3). For the superstructure, it is convenient to take such a large orthohexagonal lattice as having $a = 2A_1$, $b = 2A_1 + 4A_2$ and $c = NC$ (Fig. 4). Possible vacant positions in

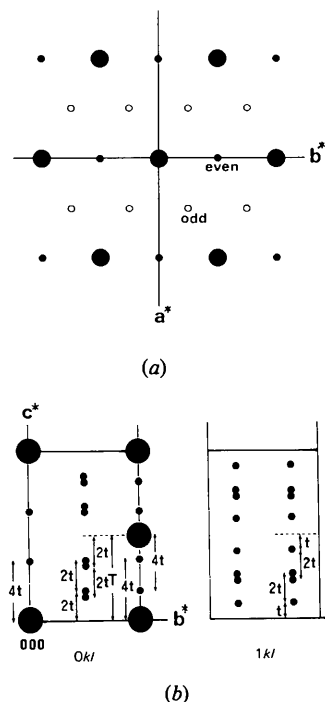


Fig. 2. Schematic diagrams of the diffraction pattern of the intermediate pyrrhotite. Large and small circles represent main and satellite reflections respectively. (a) Satellite reflections appear along the c axis. 'Odd' (open circle) and 'even' (solid circle) indicate the satellite reflections of odd and even orders respectively. (b) OkI and $1kI$ of reciprocal space. T and t represent the distances between the nearest two main reflections and between the nearest two satellite reflections. T/t is equal to N .

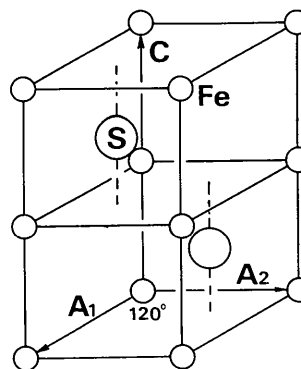


Fig. 3. The fundamental NiAs-type structure with the hexagonal cell edges of A and C .

each Fe layer parallel to (001) are reasonably assumed to have the (x,y) coordinates as follows:

$$\begin{aligned} A & (0,0) \text{ and } (\frac{1}{2}, \frac{1}{2}); \\ B & (\frac{1}{2}, \frac{1}{4}) \text{ and } (\frac{3}{4}, \frac{3}{4}); \\ C & (\frac{1}{2}, 0) \text{ and } (0, \frac{1}{2}); \\ D & (\frac{3}{4}, \frac{1}{4}) \text{ and } (\frac{1}{4}, \frac{3}{4}), \end{aligned}$$

which are also shown in Fig. 4. Therefore, four kinds of Fe row parallel to the c axis pass through the above four positions. The corresponding phase factors, α_j ($j = 1-4$), are, respectively, put equal to (A) $\alpha_1 = 1$, (B) $\alpha_2 = i^{h+k}$, (C) $\alpha_3 = (-1)^h$ and (D) $\alpha_4 = (-1)^h i^{h+k}$, whose values are listed in Table 1 for the different h and k in reciprocal space. The observed diffraction aspect of the satellite reflections is, as will be shown below, well explained by assuming that two kinds of out-of-step vectors such as $\mathbf{u}_1 = (\mathbf{a} + \mathbf{b})/4$ and $\mathbf{u}_2 = (\mathbf{a} - \mathbf{b})/4$ (Fig. 4) occur alternately at every $c/4$ or $N/2 = \tilde{M}$, where \tilde{M} is the number of Fe layers since the subcell has two Fe layers.

The out-of-step function, $\varphi(hkn)$, is represented as $\varphi = \varphi_1 + \varphi_2$, where φ_1 and φ_2 represent the step function and the boundary conditions of the step function, respectively (Kakinoki & Minagawa, 1972). Since the out-of-step function has a period of $4\tilde{M}$, the period M of the standard structure should be subject to the

relation $4v\tilde{M} = M$ (M integer), where v is the minimum positive integer to make $4v\tilde{M}$ equal to an integer M . Out-of-step functions with alternate vectors \mathbf{u}_1 and \mathbf{u}_2 form a spiral along the c axis, as shown in Figs. 4 and 5. We define φ beginning with \mathbf{u}_1 as clockwise and \mathbf{u}_2 as counterclockwise. Depending on h and k , (a), (b), (c) and (d) in Table 1, $\varphi(hkn)$ of clockwise (Fig. 6) are as follows:

(a) $\varphi_1(n) = 1$, where $n = 0, 1, 2, \dots, Q-1$, where Q is the number of Fe layers along the c axis.

$$(b) \varphi_1(n) = -\frac{4}{\pi} \sum_{m=0}^{\infty} \frac{1}{2m+1} \sin \pi \frac{(2m+1)n}{\tilde{M}},$$

if $\frac{(2m+1)n}{\tilde{M}} \neq \text{integer}.$

$$(c) \varphi_1(n) = -\frac{4}{\pi} \sum_{m=0}^{\infty} \frac{1}{2m+1} \sin \pi \frac{(2m+1)n}{2\tilde{M}},$$

Table 1. The h, k dependence of the four different Fe sites A, B, C and D

The corresponding phase factors, α_j ($j = 1, 2, 3$ and 4) are put equal to (A) $\alpha_1 = 1$, (B) $\alpha_2 = i^{h+k}$, (C) $\alpha_3 = (-1)^h$ and (D) $\alpha_4 = (-1)^{h+k}$, Q integer.

	(a)	(b)	(c)	(d)
h, k	both even		both odd	
$h+k$	$4Q$	$4Q+2$	$4Q$	$4Q+2$
α_1	1	1	1	1
α_2	1	-1	1	-1
α_3	1	1	-1	-1
α_4	1	-1	-1	1

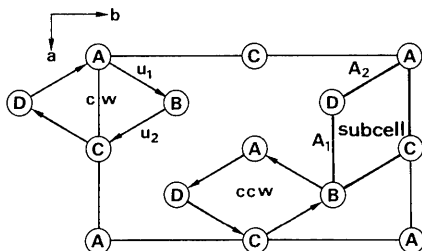


Fig. 4. Supercell of intermediate pyrrhotite with the subcell vectors of \mathbf{A}_1 and \mathbf{A}_2 . A, B, C and D represent the sites of Fe rows along the c axis in (001) of the orthohexagonal unit cell. Two different out-of-step functions which form spirals are shown: cw clockwise and ccw counterclockwise.

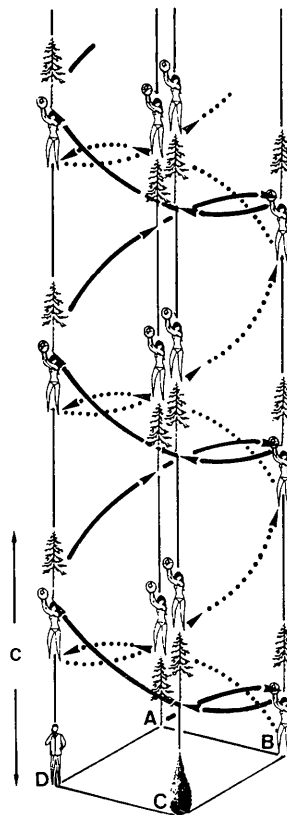


Fig. 5. Schematic diagram of two kinds of spiral in pyrrhotite. Figures which start from A and C (trees) form a clockwise spiral (solid line) and those which start from B and D (woman and man respectively) form a counterclockwise spiral (dotted line). Figures for C and D are drawn only at the starting points. The meaning of A, B, C and D is the same as in Fig. 4.

if $\frac{(2m+1)n}{2\tilde{M}} \neq \text{integer}$.

$$(d) \varphi_1(n) = \frac{4}{\pi} \sum_{m=0}^{\infty} \frac{(-1)^m}{2m+1} \cos \pi \frac{(2m+1)n}{2\tilde{M}},$$

if $\frac{(2m+1)n}{\tilde{M}} \neq \text{integer}$.

For φ counterclockwise, (a) and (b) are the same but (c) and (d) are interchanged. Boundary conditions φ_2 are described in the Appendix.

Two combinations of out-of-step functions

The same vector \mathbf{u}_1 or \mathbf{u}_2 must be applied to Fe rows at A and C (or B and D). However, either \mathbf{u}_1 or \mathbf{u}_2 can be applied at B and D (or A and C). This means that two combinations of out-of-step functions are possible in the structure.

(1) Out-of-step functions begin with \mathbf{u}_1 for A and C and with \mathbf{u}_2 for B and D or *vice versa*. That is, all four spirals which start from A, B, C and D are in the same direction (e.g. clockwise) as follows:

$A: A-B-C-D-A-B-C-D \dots$ (cw)
 $B: B-C-D-A-B-C-D-A \dots$ (cw)
 $C: C-D-A-B-C-D-A-B \dots$ (cw)
 $D: D-A-B-C-D-A-B-C \dots$ (cw).

(2) Out-of-step functions begin with the same vector \mathbf{u}_1 or \mathbf{u}_2 for all four positions A, B, C and D . In this case the two spirals which start from A and C are clockwise, while the other two, which start from B and D , are counterclockwise, or *vice versa* (Fig. 5).

$A: A-B-C-D-A-B-C-D \dots$ (cw)
 $B: B-A-D-C-B-A-D-C \dots$ (ccw)
 $C: C-D-A-B-C-D-A-B \dots$ (cw)
 $D: D-C-B-A-D-C-B-A \dots$ (ccw).

In both cases the diffraction aspect of the satellite reflections can be explained.

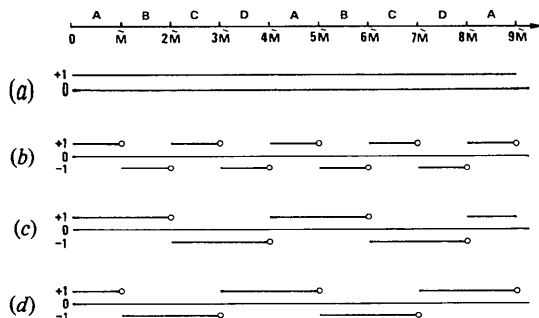


Fig. 6. Out-of-step function $\varphi(hkn)$ depending on h and k ; (a), (b), (c) and (d) in Table 1. The meaning of A, B, C and D is the same as in Fig. 4.

Distribution of Fe vacancies

Occupancy probability of Fe atoms

Let us express the Fe vacancy distribution by $p_j(n)$ ($j = 1, 2, 3$ and 4) through A, B, C and D , respectively, in the four different Fe rows along the c axis before the out-of-step vector occurs. Here n (integer) is the n th site in an Fe row and $0 \leq p_j(n) \leq 1$. It is obvious that $p_j(n)$ has a period of $\mu\tilde{M} = \tilde{M}'$ (\tilde{M}' integer) where μ is the minimum positive integer to make \tilde{M} equal to an integer \tilde{M}' . $\tilde{M}' = \tilde{M}$ if $\mu = 4$.

$p_j(n)$ is conveniently expanded as a Fourier series:

$$p_j(n) = A_0 + \sum_{m=1}^{\tilde{M}'-1} [A_m \cos(2\pi mn/\tilde{M}) + B_m \sin(2\pi mn/\tilde{M})] \quad (1)$$

where A_0, A_m and B_m are the Fourier coefficients of the j th row. Equation (1) has the following characteristics.

(i) If we use $\tilde{M}' - m$ for m , then equation (1) becomes

$$p_j(n) = A_0 + \sum_{m=1}^{\tilde{M}'-1} [A_{\tilde{M}'-m} \cos(2\pi mn/\tilde{M}) - B_{\tilde{M}'-m} \sin(2\pi mn/\tilde{M})]. \quad (2)$$

From (1) and (2), $A_{\tilde{M}'-m} = A_m$ and $B_{\tilde{M}'-m} = -B_m$. Therefore the numbers of coefficients are \tilde{M}' and $\tilde{M}' + 1$ for odd and even \tilde{M}' respectively. That is,

$\tilde{M}'; A_0, A_1, A_2, \dots, A_{(\tilde{M}'-1)/2}$ and $B_1, B_2, \dots, B_{(\tilde{M}'-1)/2}$
for \tilde{M}' odd,

and

$\tilde{M}' + 1; A_0, A_1, \dots, A_{\tilde{M}'/2}$ and $B_1, B_2, \dots, B_{\tilde{M}'/2}$
for \tilde{M}' even.

Since

$$B_{\tilde{M}'/2} \sin[2\pi(\tilde{M}'/2)n/\tilde{M}] = B_{\tilde{M}'/2} \sin \pi n = 0$$

for \tilde{M}' even, the number of coefficients to be determined is \tilde{M}' for both \tilde{M}' even and \tilde{M}' odd.

(ii) When \tilde{M} is an integer, then $\tilde{M} = \tilde{M}'$ ($\mu = 1$). If we use $\tilde{M}' + n$ for n , then

$$\cos[2\pi m(\tilde{M}' + n)/\tilde{M}'] = \cos(2\pi mn/\tilde{M}')$$

and

$$\sin[2\pi m(\tilde{M}' + n)/\tilde{M}'] = \sin(2\pi mn/\tilde{M}').$$

Therefore the period of $p(n)$, \tilde{M}' , is an integer.

Relations between the out-of-step function φ and the phase factor α of A, B, C and D sites are shown in Fig. 6. As the crystal has a C -base-centered lattice, the geometrical structure factor of the Fe vacancy, G_v , is

$$G_v = 2 \sum_{n=0}^{Q-1} p(hkn) \varphi(hkn) \exp(2\pi i n \zeta). \quad (3)$$

Here

$$p(hkn) = \sum_{j=1}^4 \alpha_j(hk) \cdot p_j(n)$$

and the parameters are based on the period of the Fe layers along the c axis. Coefficients of $p(hkn)$ are, therefore,

$$A_0 = \sum_{j=1}^4 \alpha_j \cdot A_{0j}, \quad A_m = \sum_{j=1}^4 \alpha_j A_{mj} \quad \text{and} \\ B_m = \sum_{j=1}^4 \alpha_j B_{mj}.$$

Here suffix j represents the coefficients of the j th row in Table 1.

Taking into account the phase factors in Table 1, we obtain

$$p(n) = \sum_{j=1}^4 \alpha_j p_j(n)$$

as follows:

$$p(n) \begin{cases} = p_1(n) + p_2(n) + p_3(n) + p_4(n) \text{ for (a),} \\ = p_1(n) - p_2(n) + p_3(n) - p_4(n) \text{ for (b),} \\ = p_1(n) + p_2(n) - p_3(n) - p_4(n) \text{ for (c),} \\ = p_1(n) - p_2(n) - p_3(n) + p_4(n) \text{ for (d).} \end{cases}$$

Therefore $-2 \leq p(n) \leq 4$.

Relation between A_0 and composition

The composition is represented as $\text{Fe}_{r-1}\text{S}_r$ in special cases of $r = 8$ (the 4C type), 10(5C), 11(11C) and 12(6C). Since for every composition eight Fe sites are in an Fe layer parallel to (001), $8 \times M'$ sites are in M' Fe layers. In the n th layer, the number of vacancies for Fe atoms is

$$2[p_1(n) + p_2(n) + p_3(n) + p_4(n)] = 2p(n).$$

Therefore $1/r$ is represented as

$$\frac{1}{r} = \frac{1}{8M'} \times 2 \sum_{n=0}^{M'-1} p(n) = \frac{1}{4M'} S.$$

Here

$$S = 4M'/n = \sum_{n=0}^{M'-1} p(n) \\ = \sum_{n=0}^{M'-1} \left\{ A_0 + \sum_{m=1}^{M'-1} [A_m \cos(2\pi mn/\tilde{M}) + B_m \sin(2\pi mn/\tilde{M})] \right\} \\ = A_0 M' + \sum_{m=1}^{M'-1} \left[A_m \sum_{n=0}^{M'-1} \cos(2\pi mn/\tilde{M}) + B_m \sum_{n=0}^{M'-1} \sin(2\pi mn/\tilde{M}) \right] \\ = A_0 M',$$

since

$$\sum_{n=0}^{M'-1} \cos(2\pi mn/\tilde{M}) = 1 + \cos(\pi vm) \\ \times \sin[(M' - 1)\pi vm/M'] / \sin(\pi vm/M') = 0$$

and

$$\sum_{n=0}^{M'-1} \sin(2\pi mn/\tilde{M}) = \sin(\pi vm) \\ \times \sin[(M' - 1)\pi vm/M'] / \sin(\pi vm/M') = 0.$$

Let us express the average number of vacancies in each Fe row at A , B , C and D sites before the out-of-step vector occurs as r_1 , r_2 , r_3 and r_4 respectively, which represent

$$r_1 = \frac{2}{M'} \sum_{n=0}^{M'-1} p_1(n), \quad r_2 = \frac{2}{M'} \sum_{n=0}^{M'-1} p_2(n), \text{ etc.}$$

Then coefficient A_0 and the composition are related as follows:

$$A_0 = \frac{S}{M'} = \frac{1}{M'} \sum_{n=0}^{M'-1} p(n) \\ = \frac{1}{M'} \sum_{n=0}^{M'-1} [p_1(n) + p_2(n) + p_3(n) + p_4(n)] \\ = (r_1 + r_2 + r_3 + r_4)/2 = 4/r \text{ for (a).}$$

Similarly we obtain

$$A_0 \begin{cases} = (r_1 - r_2 + r_3 - r_4)/2 \text{ for (b),} \\ = (r_1 + r_2 - r_3 - r_4)/2 \text{ for (c),} \\ = (r_1 - r_2 - r_3 + r_4)/2 \text{ for (d).} \end{cases}$$

Application to the 4C-, 5C- and 6C-type structures

In the 4C-type (Fe_7S_8) (Bertaut, 1953) and 6C-type ($\text{Fe}_{11}\text{S}_{12}$) (Koto, Morimoto & Gyobu, 1975) structures, the Fe vacancies are completely ordered in an Fe layer parallel to (001), but the stacking sequence of the ordered layers is different. The distribution of the Fe vacancies in both structures is described by an occupancy probability function [for example $p_1(n)$] and the other three functions have zero value. As understood from Fig. 1 (the same as Fig. 5 of Koto, Morimoto & Gyobu, 1975), $p_1(n)$ of the 4C and 6C types is described as follows.

For the 4C type

$$N = 4, \quad \tilde{M} = N/2 = 2 \quad \text{and} \quad M' = \mu\tilde{M} = 2(\mu = 1).$$

Equation (1) becomes

$$p_1(n) = A_0 + \sum_{m=1}^{2-1} [A_m \cos(2\pi mn/\tilde{M}) + B_m \sin(2\pi mn/\tilde{M})] \\ = A_0 + A_1 \cos(2\pi n/2) + B_1 \sin(2\pi n/2) \\ = A_0 + A_1 \cos(\pi n).$$

From the relation between A_0 and the composition,

$$A_0 = 4/r = 1/2.$$

As $p_1(n)$ is represented as

$$0 \ 1 \ 0 \ 1 \ 0 \ 1 \ 0 \ 1 \dots, \quad p_1(0) = 1/2 + A_1 = 0.$$

Therefore $A_1 = -1/2$. We obtain

$$p_1(n) = 1/2 - \cos(\pi n)/2.$$

For the 6C type

$$N = 6, \quad \tilde{M} = N/2 = 3 \quad \text{and} \quad M' = \mu\tilde{M} = 3(\mu = 1).$$

$$\begin{aligned} p_1(n) &= A_0 + \sum_{m=1}^{3-1} [A_m \cos(2\pi mn/\tilde{M}) \\ &\quad + B_m \sin(2\pi mn/\tilde{M})] \\ &= A_0 + A_1 \cos(2\pi n/2) + A_2 \cos(2\pi \times 2n/3) \\ &\quad + B_1 \sin(2\pi n/3) + B_2 \sin(2\pi \times 2n/3) \\ &= A_0 + 2A_1 \cos(\pi n/3) - 2B_1 \sin(\pi n/3) \end{aligned}$$

since $A_1 = A_2$ and $B_1 = -B_2$; $A_0 = 1/3$.

As $p_1(n)$ is represented as

$$\begin{aligned} 0 \ 1/2 \ 1/2 \ 0 \ 1/2 \ 1/2 \ 0 \ 1/2 \ 1/2 \ 0 \dots, \\ p_1(0) = 1/3 + 2A_1 = 0 \end{aligned}$$

and

$$p_1(1) = 1/3 + 2A_1 \cos(\pi/3) - 2B_1 \sin(\pi/3) = 1/2.$$

Therefore $A_1 = -1/6$ and $B_1 = 0$. We obtain

$$p_1(n) = 1/3 - \cos(\pi n/3)/3.$$

For the 5C type

$$N = 5, \quad \tilde{M} = N/2 = 2.5 \quad \text{and} \quad M' = \mu\tilde{M} = 5(\mu = 2).$$

Although the structure of the 5C type is unknown, $p_1(n)$ is described as follows, if it is assumed that $p_1(n)$ has non-zero value and the other three functions have zero value, as in the 4C and 6C types:

$$\begin{aligned} p_1(n) &= A_0 + \sum_{m=1}^{5-1} [A_m \cos(2\pi mn/\tilde{M}) \\ &\quad + B_m \sin(2\pi mn/\tilde{M})] \\ &= A_0 + A_1 \cos(2\pi n/2.5) + A_2 \cos(2\pi \times 2n/2.5) \\ &\quad + A_3 \cos(2\pi \times 3n/2.5) \\ &\quad + A_4 \cos(2\pi \times 4n/2.5) \\ &\quad + B_1 \sin(2\pi n/2.5) + B_2 \sin(2\pi \times 2n/2.5) \\ &\quad + B_3 \sin(2\pi \times 3n/2.5) \\ &\quad + B_4 \sin(2\pi \times 4n/2.5) \\ &= A_0 + 2A_1 \cos(6\pi n/5) + 2A_2 \cos(2\pi n/5) \\ &\quad - 2B_1 \sin(6\pi n/5) - 2B_2 \sin(2\pi n/5), \end{aligned}$$

since $A_1 = A_4$, $A_2 = A_3$, $B_1 = -B_4$ and $B_2 = -B_3$; $A_0 = 4/r = 2/5$. We obtain

$$\begin{aligned} p_1(n) &= 2/5 + 2A_1 \cos(6\pi n/5) + 2A_2 \cos(2\pi n/5) \\ &\quad - 2B_1 \sin(6\pi n/5) - 2B_2 \sin(2\pi n/5). \end{aligned}$$

Thus the distribution of Fe vacancies in the 5C type is described by the above function with four coefficients A_1 , A_2 , B_1 and B_2 . The structure of the 5C type is studied elsewhere.

Geometrical structure factor of Fe vacancies

Since main and satellite reflections are sharp and not diffuse, only the Laue peak is taken into consideration in the calculation of the geometrical structure factor due to the distribution of Fe vacancies. The calculation is made by taking the Fe vacancies only into account as for the 6C type (Koto, Morimoto & Gyobu, 1975). Boundary conditions φ_2 of out-of-step functions are omitted in the following calculations.

Equation (3) becomes as follows, depending on h and k ; (a), (b), (c) and (d) are as in Table 1:

$$\begin{aligned} (a) \ G_v &= 2 \sum_{n=0}^{Q-1} p(n) \exp(2\pi i n \zeta) \\ &= 2 \left\{ A_0 \sum_{n=0}^{Q-1} \exp(2\pi i n \zeta) \right. \\ &\quad + \sum_{m=1}^{M'-1} [A_m \sum_{n=0}^{Q-1} \cos(2\pi mn/\tilde{M}) \exp(2\pi i n \zeta) \\ &\quad + B_m \sum_{n=0}^{Q-1} \sin(2\pi mn/\tilde{M}) \exp(2\pi i n \zeta)] \Big\} \\ &= Q \left\{ 2A_0 \delta_{\zeta, L} + \sum_{m=1}^{M'-1} [A_m (\delta_{\zeta, L-m/\tilde{M}} \right. \\ &\quad + \delta_{\zeta, L+m/\tilde{M}}) - iB_m (\delta_{\zeta, L-m/\tilde{M}} - \delta_{\zeta, L+m/\tilde{M}})] \Big\}. \end{aligned}$$

Therefore

$$G_v = \begin{cases} = 2QA_0 \delta_{\zeta, L} & \text{when } h, k \text{ and } \zeta = L, \\ = Q(A_m + iB_m) \delta_{\zeta, L+m/\tilde{M}} & \text{when } h, k \text{ and } \\ & \zeta = L + m/\tilde{M} \\ = Q(A_m - iB_m) \delta_{\zeta, L-m/\tilde{M}} & \text{when } h, k \text{ and } \\ & \zeta = L - m/\tilde{M}, \end{cases}$$

where $m = 1, 2, \dots, M' - 1$.

$$\begin{aligned}
(b) \ G_v &= 2 \sum_{n=0}^{Q-1} \left[A_0 + \sum_{m=1}^{M'-1} \left(A_m \cos 2\pi \frac{2m}{2\tilde{M}} n \right. \right. \\
&\quad \left. \left. + B_m \sin 2\pi \frac{2m}{2\tilde{M}} n \right) \right] \\
&\quad \times \left[\frac{4}{\pi} \sum_{m'=0}^{\infty} \frac{1}{2m'+1} \sin 2\pi \frac{2m'+1}{2\tilde{M}} n \right] \\
&\quad \times \exp(2\pi i n \zeta) \\
&= \frac{2Q}{\pi} \sum_{m'=0}^{\infty} \frac{1}{2m'+1} \left\{ 2iA_0 (\delta_{\zeta, L+(2m'+1)/2\tilde{M}} \right. \\
&\quad - \delta_{\zeta, L-(2m'+1)/2\tilde{M}}) \\
&\quad + \sum_{m=1}^{M'-1} [(iA_m - B_m) \delta_{\zeta, L+[2(m+m')+1]/2\tilde{M}} \\
&\quad - (iA_m + B_m) \delta_{\zeta, L-[2(m+m')+1]/2\tilde{M}} \\
&\quad + (iA_m + B_m) \delta_{\zeta, L+[2(m'-m)+1]/2\tilde{M}} \\
&\quad \left. - (iA_m - B_m) \delta_{\zeta, L-[2(m'-m)+1]/2\tilde{M}}] \right\}. \\
(c) \ G_v &= 2 \sum_{n=0}^{Q-1} \left[A_0 + \sum_{m=1}^{M'-1} \left(A_m \cos 2\pi \frac{4m}{4\tilde{M}} n \right. \right. \\
&\quad \left. \left. + B_m \sin 2\pi \frac{4m}{4\tilde{M}} n \right) \right] \\
&\quad \times \left[\frac{4}{\pi} \sum_{m'=0}^{\infty} \frac{1}{2m'+1} \sin 2\pi \frac{2m'+1}{4\tilde{M}} n \right] \\
&\quad \times \exp(2\pi i n \zeta) \\
&= \frac{4Q}{\pi} \left\{ 4iA_0 \sum_{m'=0}^{\infty} \frac{1}{2m'+1} (\delta_{\zeta, L+(2m'+1)/4\tilde{M}} \right. \\
&\quad - \delta_{\zeta, L-(2m'+1)/4\tilde{M}}) \\
&\quad + \sum_{m=1}^{M_0-1} \left[2(iA_m - B_m) \right. \\
&\quad \times \sum_{m'=0}^{\infty} \frac{1}{2m'+1} \delta_{\zeta, L+[2(m'+2m)+1]/4\tilde{M}} \\
&\quad - 2(iA_m + B_m) \\
&\quad \times \sum_{m'=0}^{\infty} \frac{1}{2m'+1} \delta_{\zeta, L-[2(m'+2m)+1]/4\tilde{M}} \\
&\quad + 2(iA_m + B_m) \\
&\quad \times \sum_{m'=0}^{\infty} \frac{1}{2m'+1} \delta_{\zeta, L+[2(m'-2m)+1]/4\tilde{M}} \\
&\quad - 2(iA_m - B_m) \\
&\quad \left. \times \sum_{m'=0}^{\infty} \frac{1}{2m'+1} \delta_{\zeta, L-[2(m'-2m)+1]/4\tilde{M}} \right] \Bigg\}.
\end{aligned}$$

$$\begin{aligned}
(d) \ G_v &= 2 \sum_{n=0}^{Q-1} \left[A_0 + \sum_{m=1}^{M'-1} \left(A_m \cos 2\pi \frac{4m}{4\tilde{M}} n \right. \right. \\
&\quad \left. \left. + B_m \sin 2\pi \frac{4m}{4\tilde{M}} n \right) \right] \\
&\quad \times \left[\frac{4}{\pi} \sum_{m'=0}^{\infty} \frac{(-1)^m}{2m'+1} \cos 2\pi \frac{2m'+1}{4\tilde{M}} n \right] \\
&\quad \times \exp(2\pi i n \zeta) \\
&= \frac{4Q}{\pi} \left\{ 4A_0 \sum_{m'=0}^{\infty} \frac{(-1)^{m'}}{2m'+1} (\delta_{\zeta, L-(2m'+1)/4\tilde{M}} \right. \\
&\quad + \delta_{\zeta, L+(2m'+1)/4\tilde{M}}) \\
&\quad + \sum_{m=1}^{M'-1} \left[2(A_m + iB_m) \sum_{m'=0}^{\infty} \frac{(-1)^{m'}}{2m'+1} \right. \\
&\quad \times \delta_{\zeta, L+[2(m'+2m)+1]/4\tilde{M}} \\
&\quad + 2(A_m - iB_m) \sum_{m'=0}^{\infty} \frac{(-1)^{m'}}{2m'+1} \\
&\quad \times \delta_{\zeta, L-[2(m'+2m)+1]/4\tilde{M}} \\
&\quad + 2(A_m - iB_m) \sum_{m'=0}^{\infty} \frac{(-1)^{m'}}{2m'+1} \\
&\quad \times \delta_{\zeta, L+[2(m'-2m)+1]/4\tilde{M}} \\
&\quad + 2(A_m + iB_m) \sum_{m'=0}^{\infty} \frac{(-1)^{m'}}{2m'+1} \\
&\quad \left. \left. \times \delta_{\zeta, L-[2(m'-2m)+1]/4\tilde{M}} \right] \right\}.
\end{aligned}$$

To sum up, satellite reflections due to distribution of Fe vacancies can be found at $L \pm (u/\tilde{M})$ (L and u integer) referred to the subcell of Fe atoms along a reciprocal row (a) in Table 1, at $L \pm (2u+1)/2\tilde{M}$ along row (b) and $L \pm (2u+1)/4\tilde{M}$ along rows (c) and (d). That is, along (a) only fourth-order satellite reflections, along row (b) only second-order (mod 4), and along (c) and (d) only odd orders can have non-zero values of G_v . The results also indicate that G_v is the same for the same order of satellite reflections. Furthermore, it is understood from G_v that satellite reflections of the same order in each row have the same intensity, $G_v G_v^*$, and those for (c) and (d) rows also have the same, resulting in three different rows, (a), (b) and (c) = (d).

In the calculation of intensity by using the above formulae for geometrical structure factors, it must be noted that, if two and more satellite reflections appear at the same reciprocal point, the intensity must be calculated by squaring the sum of all structure factors and not by summing all intensities. This is the case, for example, for M' integer, e.g. the 4C, 5C and 6C types.

Discussion

Displacements of atoms

Displacements of Fe and S atoms may occur, followed by the ordering of Fe vacancies in the fundamental NiAs-type structure. Therefore contributions, due both to ordering of Fe vacancies and to displacements of Fe and S atoms, are observed in the intensity of satellite reflections. Satellite reflections due to displacements of atoms appear based on the cell edges of the fundamental NiAs-type and not on those of the Fe subcell. To determine the distribution of Fe vacancies, the intensity due only to the vacancy distribution is obtained by extrapolating the intensity average of satellite reflections of the same kinds to $(\sin \theta/\lambda) = 0$. In this way, intensity due to displacements of atoms in the fundamental NiAs-type structure can be excluded and that due to vacancy distribution can be obtained, as in the structure determination of the 6C type (Koto, Morimoto & Gyobu, 1975).

Magnetic properties

The strong ferrimagnetic property of the 4C type is interpreted in terms of the ordered structure of the Fe vacancies with alternate layers Fe Filled (*F*) and Fe defective (*D*) (Bertaut, 1953). Attempts to interpret the antiferromagnetic property of the intermediate pyrrhotite were made on the basis of the same concepts as for the 4C type with models of a completely ordered structure of Fe vacancies (e.g. Schwarz & Vaughan, 1972). However, X-ray structure analysis of the 6C type resulted in the disordered structure, which is interpreted as forming a domain texture. In the domain model of Koto, Morimoto & Gyobu (1975), there exists the sequence unit of the five Fe layers, *FDFDF*, which is part of the structure of the 4C type. The sequence unit must show a ferrimagnetic property. As the 6C type consists of the same number of units with opposite orientation to the ferrimagnetic domain, there will be a cancellation of the magnetic moment and antiferromagnetism will result. The same concepts can be applied for interpretation of the antiferromagnetism of the intermediate pyrrhotite.

Disorder in an Fe layer at elevated temperatures

With increasing temperature, the value of *N* decreases for the same composition; e.g. a value of 6 at room temperature for Fe₁₁S₁₂ decreases continuously to 3 just below transition temperature to the high-temperature form of the 1C type (Nakazawa & Morimoto, 1971). It is reasonable to consider that the disordered state occurs at elevated temperatures, i.e. some Fe atoms leave an Fe row parallel to the *c* axis and go to one of the other three Fe rows, resulting in more vacancies in the first Fe row. This indicates that not only one Fe row but also any of the other three Fe

rows can have non-zero value; i.e. there is disorder in an Fe layer parallel to (001).

Conclusions

The diffraction aspect of the incommensurate intermediate pyrrhotite has been explained by a one-dimensional out-of-step function which occurs at every quarter of the *c* period, as in the commensurate structures of Fe₇S₈ and Fe₁₁S₁₂. The satellite reflections can be principally attributed to the distribution of Fe vacancies, which is conveniently expanded as a Fourier series. The relationships between coefficients of the Fourier series have been obtained.

The authors express their sincere thanks to Professor J. Kakinoki, Setsunan University, for his helpful comments and useful discussions, which improved the manuscript. They also thank Dr M. Tokonami of this Institute for his critical discussions and Professor N. Morimoto, Kyoto University, for his interest in this problem.

APPENDIX

Boundary conditions of the step function

(a) No boundary condition.

$$(b) \varphi_2(n) = \sum_{p=0} (\delta_{n,2p\tilde{M}} - \delta_{n,(2p+1)\tilde{M}}) \\ \text{if } \frac{(2m+1)n}{\tilde{M}} \text{ integer,}$$

where δ is the Kronecker delta function (with *p* integer).

$$(c) \varphi_2(n) = \sum_{p=0} (\delta_{n,2p \times 2\tilde{M}} - \delta_{n,(2p+1) \times 2\tilde{M}}) \\ \text{if } \frac{(2m+1)n}{2\tilde{M}} \text{ integer.}$$

$$(d) \varphi_2(n) = \sum_{p=0} (\delta_{n,(4p+3)\tilde{M}} - \delta_{n,(4p+1)\tilde{M}}) \\ \text{if } \frac{(2m+1)n}{\tilde{M}} \text{ integer.}$$

References

- BERTAUT, E. F. (1953). *Acta Cryst.* **6**, 557–561.
- FUJIWARA, K. (1957). *J. Phys. Soc. Jpn.* **12**, 7–13.
- KAKINOKI, J. & MINAGAWA, T. (1972). *Acta Cryst.* **A28**, 120–133.
- KOTO, K., MORIMOTO, N. & GYOBU, A. (1975). *Acta Cryst.* **B31**, 2759–2674.
- KOTO, K., MORIMOTO, N. & KITAMURA, M. (1975). *Acta Cryst.* **A31**, S86.
- MINAGAWA, T. (1972). *Acta Cryst.* **A28**, 308–318.
- MORIMOTO, N., GYOBU, A., TSUKUMA, K. & KOTO, K. (1975). *Am. Mineral.* **77**, 234–260.
- NAKAZAWA, H. & MORIMOTO, N. (1971). *Mater. Res. Bull.* **6**, 345–358.
- SCHWARZ, E. J. & VAUGHAN, D. J. (1972). *J. Geomagn. Geoelectr.* **24**, 441–458.